

Contents

1.	The Jamming Transition and the Marginally Stable Solid	1
	<i>F. Arceri, E. I. Corwin, C. S. O’Hern</i>	
1.1	Introduction	1
1.2	Jamming Criticality	3
1.3	Marginal Stability	5
1.4	Numerical Confirmations of the Mean-Field Theory of Jamming	8
1.5	Experimental Validations of the Mean-Field Theory of Jamming	12
1.6	Beyond Sphere Packings	13
1.7	Acknowledgements	18
	<i>Bibliography</i>	21

Chapter 1

The Jamming Transition and the Marginally Stable Solid

Francesco Arceri¹, Eric I. Corwin², Corey S. O'Hern^{1, 3, 4}

¹*Department of Mechanical Engineering and Materials Science, Yale University, New Haven, Connecticut 06511, USA*

²*Department of Physics and Materials Science Institute, University of Oregon, Eugene, Oregon 97403, USA*

³*Department of Physics, Yale University, New Haven, Connecticut 06511, USA*

⁴*Department of Applied Physics, Yale University, New Haven, Connecticut 06511, USA*

1.1 Introduction

Few things in this world are as common as earth, dirt, and sand. And yet, even as the most exotic, the most distant, and the smallest objects in our universe have fallen prey to human understanding, the nature and origin of the structural and mechanical properties of these materials has been, until recently, surprisingly resistant. It was not for a lack of trying. The *jamming* transition, by which a collection of macroscopic particles goes from flowing to rigid, lies not only at the heart of building practices throughout human history, but is ubiquitous in everyday life. Examples range from grains poured into a container [Behringer and Chakraborty(2019)], to foams and emulsions in foods such as ice cream and mayonnaise [van Hecke(2010)], and to sand piles and gravel at the beach and in city parks [Cates *et al.*(1998)Cates, Wittmer, Bouchaud and Claudin]. The jamming transition from fluid-to-solid behavior in these different systems shares a fundamental feature: the energy scale of the interaction between particles is sufficiently large that thermal fluctuations at room temperature

are far too small to affect the dynamics. The control parameters of the jamming transition are therefore the external pressure exerted on the system and the volume in which the system is confined. The first academic study of jamming dates to 1727, when Reverend Steven Hales studied the structures formed by the contacts between dried peas, compressed in an iron pot [Hales *et al.*(1727)Hales, Gribelin, Innys, Innys, Woodward, Innys and Woodward]. Such luminaries as Isaac Newton [Newton(1848)] and James Clerk Maxwell [Maxwell(1864)] attempted to analytically solve for the properties of jammed packings, but were only able to determine bounds on number of contacts per particle required for mechanical stability. More recently, Bernal connected the amorphous geometric structure of spheres to the properties of the liquid state of matter [Bernal(1960)]. However, it was not until nearly the turn of this century that the modern study of jamming was initiated [Wittmer *et al.*(1996)Wittmer, Claudin, Cates and Bouchaud; de Gennes(1999); Tkachenko and Witten(1999)]. Particularly, Liu and Nagel [Liu and Nagel(1998)] made the critical realization that athermal jamming could be united with another age old problem: the glass transition. Only within the last decade has a first-principles description of jamming transition seemed possible, enabled by insights from the mean-field theory of glasses and jamming [Parisi *et al.*(2020)Parisi, Urbani and Zampori]. Because in this framework the jamming transition takes place within a full replica symmetry breaking (RSB) phase [Mézard *et al.*(1984)Mézard, Parisi, Sourlas, Toulouse and Virasoro], this seemingly simple problem has revealed a world of amazing complexity.

Recent developments in the physics of the glass transition have led to groundbreaking results in the field of jamming. Although the glass transition signals a drastic (and markedly distinct) dynamical slowdown upon cooling, both transitions can be observed in systems of hard particles, which do not deform during collisions. The simple *hard-sphere* model, in particular, has offered theoretical physicists fertile ground for building a mean-field theory of glasses, with jamming occurring in the limit of infinite pressure. Despite the great advances that the hard-sphere model has brought to the field, the fact that it has a discontinuous inter-particle potential represents a major obstacle for computing the mechanical properties in finite-dimensional systems. As a remedy, soft-sphere models, where particle deformations are described by shared volume between particles, have been used in the field as they allow more direct calculations of inter-particle forces. The fact that the jamming transition for frictionless spherical particles can be studied using both the hard- and soft-particle models reflects

its geometrical nature. By considering the average number of contacts per particle, z , one finds that the jamming of hard and soft spheres occurs at $z_c = 2d$ [Maxwell(1864)], i.e., the minimum number of contacts to ensure rigidity [O'Hern *et al.*(2002)O'Hern, Langer, Liu and Nagel] (Maxwell's criterion). For soft spheres, which can be compressed beyond the jamming point, the excess number of contacts scales as:

$$\Delta z \equiv z - z_c \sim \Delta\varphi^{1/2}, \quad (1.1)$$

where φ is the packing fraction and the excess packing fraction $\Delta\varphi = \varphi - \varphi_J$ represents the amount of compression above the jamming threshold, which is itself protocol dependent [Durian(1995); O'Hern *et al.*(2003)O'Hern, Silbert, Liu and Nagel]. Further, several studies have shown an exact correspondence in the inter-particle separations between jammed hard-particle and soft-particle packings [O'Hern *et al.*(2003)O'Hern, Silbert, Liu and Nagel; Donev *et al.*(2005)Donev, Torquato and Stillinger], confirming that accessible configurations of hard and soft spheres are identical near jamming onset [Brito and Wyart(2006); Wu *et al.*(2017)Wu, Bertrand, Shattuck and O'Hern; Arceri and Corwin(2020)].

1.2 Jamming Criticality

Many numerical studies have documented critical behaviors of bulk quantities near the jamming transition, including observation of power-law scaling [O'Hern *et al.*(2002)O'Hern, Langer, Liu and Nagel; O'Hern *et al.*(2003)O'Hern, Silbert, Liu and Nagel; Ellenbroek *et al.*(2009)Ellenbroek, van Hecke and van Saarloos], scaling collapse of the elastic moduli and excess contact number [Ellenbroek *et al.*(2006)Ellenbroek, Somfai, van Hecke and van Saarloos; Dagois-Bohy *et al.*(2012)Dagois-Bohy, Tighe, Simon, Henkes and van Hecke; Goodrich *et al.*(2014)Goodrich, Dagois-Bohy, Tighe, van Hecke, Liu and Nagel; van Deen *et al.*(2014)van Deen, Simon, Zeravcic, Dagois-Bohy, Tighe and van Hecke], identification of diverging length scales [Silbert *et al.*(2005)Silbert, Liu and Nagel; Wyart *et al.*(2005)Wyart, Nagel and Witten; Goodrich *et al.*(2013)Goodrich, Ellenbroek and Liu; Lerner *et al.*(2014)Lerner, DeGiuli, Düring and Wyart], and analyses of finite-size scaling [Goodrich *et al.*(2014)Goodrich, Dagois-Bohy, Tighe, van Hecke, Liu and Nagel]. Recent studies have unified these scaling relations in a single theory of jamming using a *scaling ansatz* [Goodrich *et al.*(2016)Goodrich, Liu and Sethna]. This approach borrows ideas from critical phenomena, such

as spontaneous magnetization and density-charge waves [Widom(1965); Middleton and Fisher(1993); Pázmándi *et al.*(1997)Pázmándi, Scalettar and Zimányi], to describe scaling relations for the energy E , pressure p , excess packing fraction $\Delta\varphi$, shear stress s , shear strain ϵ , bulk modulus B , shear modulus G , and number of particles N obtained from a single state function for the elastic energy

$$E(\Delta Z, \Delta\varphi, \epsilon, N) = \Delta Z^\zeta \mathcal{E}_0 \left(\frac{\Delta\varphi}{\Delta Z^{\beta_\varphi}}, \frac{\epsilon}{\Delta Z^{\beta_\epsilon}}, N \Delta Z^\psi \right) \quad (1.2)$$

and its derivatives

$$p \equiv \varphi \frac{dE}{d\Delta\varphi}, \quad s \equiv \epsilon \frac{dE}{d\epsilon}, \quad B \equiv \frac{\varphi^2}{2} \frac{d^2 E}{d\Delta\varphi^2}, \quad G \equiv \frac{d^2 E}{d\epsilon^2}. \quad (1.3)$$

Notice that $\Delta Z = N\Delta z$ is the total number of excess contacts in a jammed soft-sphere system. These relations yield a set of equations that couple the critical exponents. The picture is completed by the addition of the *pressure-shear stress exponent equality*, which dictates that s^2 vanishes in the infinite-size limit as $1/N$.

Although the scaling ansatz offers a description in the $\Delta\varphi\epsilon N$ ensemble, numerical studies are often conducted in the $p\epsilon N$ or psN ensembles as both pressure and shear stress vanish at the jamming point. The scaling ansatz can be extended to the psN ensemble at finite temperature by defining a new state function for the free energy:

$$F(\Delta Z, p, s, N, T) = \Delta Z^\zeta \mathcal{F}_0 \left(\frac{p}{\Delta Z^{\delta_p}}, \frac{s}{\Delta Z^{\delta_s}}, N \Delta Z^\psi, \frac{T}{\Delta Z^{\delta_T}} \right). \quad (1.4)$$

The new scaling exponent equation, $\delta_T = \zeta = 4$, is consistent with the scaling of the critical temperature, $T^* \simeq \Delta Z^4$, which defines the separation between glass and jamming-like behavior [Ikeda *et al.*(2013)Ikeda, Berthier and Biroli; Wu *et al.*(2017)Wu, Bertrand, Shattuck and O'Hern]. A scaling theory for thermal systems is nevertheless far from complete due to glassy phenomena, such as aging and dynamical heterogeneity, which stem from the temperature-activated breaking and reformation of particle contacts, that is difficult to capture with simple scaling laws [Brito and Wyart(2009); Schreck *et al.*(2011)Schreck, Bertrand, O'Hern and Shattuck].

The scaling ansatz provides a framework that connects the structural and mechanical properties (ΔZ and G) for particle systems above the onset of jamming. The existence of such a framework implies that the jamming transition exhibits scaling invariance, a helpful tool for a renormalization group description. However, recent studies of the shear modulus near the

jamming transition have highlighted the limits of the scaling ansatz [VanderWerf *et al.*(2020)VanderWerf, Boromand, Shattuck and O'Hern; Wang *et al.*(2021b)Wang, Zhang, Tuckman, Ouellette, Shattuck and O'Hern]. In particular, the scaling ansatz cannot explain why the shear modulus G scales linearly with ΔZ , a result which has been numerically tested and theoretically confirmed by effective medium theory [Wyart(2010); DeGiuli *et al.*(2015)DeGiuli, Lerner and Wyart]. Interestingly, the inter-particle force law does not play a more important role in determining the shear modulus in jammed packings at non-zero pressure. In addition, the scaling analysis cannot quantify deviations between the ensemble average and the large-system limit, and it does not describe local fluctuations in the elastic moduli, or that the local elastic moduli can become negative [Dagois-Bohy *et al.*(2012)Dagois-Bohy, Tighe, Simon, Henkes and van Hecke; Wang *et al.*(2021b)Wang, Zhang, Tuckman, Ouellette, Shattuck and O'Hern]. The importance of fluctuations in the elastic moduli suggest that we need to develop a deeper understanding of the energy landscape of jammed packings.

1.3 Marginal Stability

Jammed packings are *isostatic* and marginally stable. In other words, they possess the minimum number of contacts to ensure mechanical stability and single bond-breaking perturbations can destabilize the entire system [Wyart(2012)]. Numerical and experimental studies have characterized marginal stability by measuring the vibrational density of states (VDOS) of jammed solids at finite pressure [Liu and Nagel(2010)] (Fig. 1.1). In particular, the low-frequency region of the VDOS possesses *soft modes*, i.e., low-frequency normal modes of vibration that are spatially extended and involve a large fraction of particles in the system. Upon decreasing the pressure of jammed soft spheres toward the unjamming transition, the number of force-bearing contacts decreases until it reaches the isostatic value, $N_{iso} = Nz/2$, where the number of contacts equals the number of constraints. Here, the low-frequency region of the VDOS develops a plateau and the frequency of the lowest mode scales as $\omega_c \sim \Delta\varphi^{1/2}$. Finite-size scaling shows that $\omega_c \rightarrow 0$ in the large-system limit, in which case, the soft modes correspond to zero-energy modes.

A real-space interpretation of marginal stability is offered by the so-called *cutting argument* introduced by Wyart, *et al.* [Wyart *et al.*(2005)Wyart, Nagel and Witten]. Imagine removing contacts on the

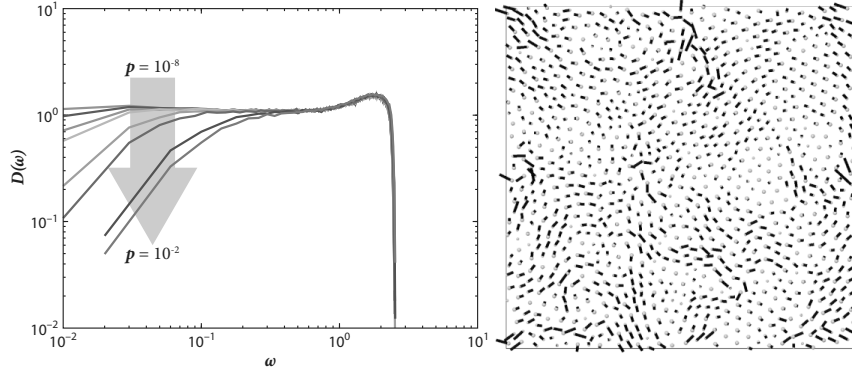


Fig. 1.1 (a) Vibrational density of states $D(\omega)$ plotted as a function of pressure p and (b) the real-space representation of a soft, extended mode. Figures reproduced with permission from Ref. [Silbert *et al.*(2005)Silbert, Liu and Nagel] ©(2005) American Physical Society.

edge between a subsystem of linear size l and the rest of the system. If at this point the system is slightly compressed, the lack of contacts leads to a competition between the overall excess contacts ΔZ created by the compression and the missing contacts at the boundary. If the total number of contacts is equal to the isostatic value N_{iso} , the system possesses soft modes. The number of soft modes N_{soft} corresponds to the difference between the number of contacts at the boundary, which are proportional to l^{d-1} , and the number of extra contacts created by the compression, which scales as $\Delta Z l^d$. Therefore, a critical length $l^* \sim \Delta \varphi^{-1/2}$ exists, below which the system is isostatic and possesses soft modes.

The mean-field theory of glasses provides a theoretical understanding of marginal stability in jammed solids as the jamming transition is viewed as the end-line of the glass phase diagram [Parisi *et al.*(2020)Parisi, Urbani and Zamponi] pictured in Fig. 1.2. Here, compression of an equilibrium liquid composed of hard spheres gives rise to dynamical arrest when the system becomes confined to one of the basins of the complex and hierarchically organized free-energy landscape. Adopting the *state-following formalism* developed by Rainone *et al.* [Rainone and Urbani(2016)], each glass state undergoes a Gardner transition upon further compression that brings the system to a marginal glass state [Berthier *et al.*(2019)Berthier, Biroli, Charbonneau, Corwin, Franz and Zamponi]. Here, the free-energy basins are fragmented into multiple sub-basins that are in turn fractured into sub-sub-basins *ad infinitum*. These marginal glass states are separated

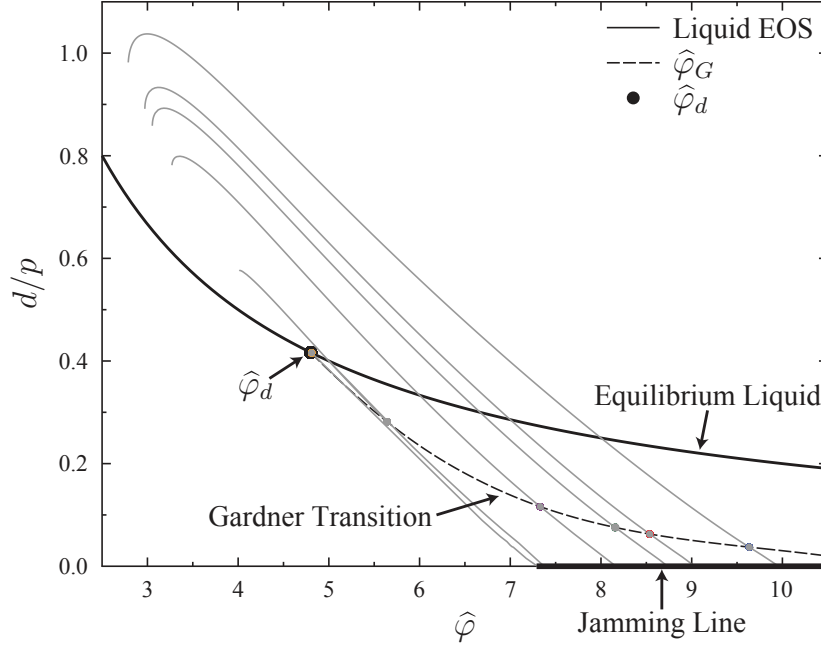


Fig. 1.2 Glass phase diagram in the d/p versus $\hat{\varphi}$ plane, where $\hat{\varphi} = 2^d \varphi/d$, φ is the packing fraction, and d is the spatial dimension. In contrast to the *equilibrium liquid* equation of state (thick solid line), each thin solid line represents a state-following compression that starts from a liquid state and evolves toward the glass and RSB glass (dotted line) regions. The end-point of each state-following compression occurs on the jamming line. Figure reproduced with permission from Ref. [Rainone and Urbani(2016)] ©(2016) IOP Publishing.

by free-energy barriers that grow with system size and link glass formation with marginally stable packings typical of jammed materials. The mean-field theory of glasses also predicts the existence of a *jamming line*, i.e., marginal glass states that cannot be further compressed occur over a range of packing fractions, which depends on the protocol used to produce the initial glass state.

Another connection between jamming and the mean-field theory of glasses is the unjamming transition of soft spheres. Finding configurations of d -dimensional spheres with no inter-particle overlaps is a type of *satisfiability problem* [Biere *et al.*(2009)Biere, Heule and van Maaren; Mézard and Montanari(2009); Franz *et al.*(2017)Franz, Parisi, Sevelev, Urbani and Zamponi]. Determining whether collections of spherical particles overlap each other can be cast as a constraint satisfaction problem,

where N variables can be adjusted to satisfy M constraints. Several algorithms have been used to solve constraint satisfaction problems, such as gradient descent [Aluffi-Pentini *et al.*(1988)Aluffi-Pentini, Parisi and Zirilli; Chacko *et al.*(2019)Chacko, Sollich and Fielding], simulated annealing [Kirkpatrick(1984)], and the perceptron model [Franz and Parisi(2016); Altieri(2018)]. The perceptron model has been successful in describing the high-dimensional energy landscape near the jamming transition [Franz *et al.*(2019)Franz, Hwang and Urbani]. In short, it describes a tracer particle on an N -dimensional hypersphere of radius \sqrt{N} with M obstacles in random positions placed on the hypersphere surface. The solution for the accessible configurations of the tracer particle maps onto the satisfiability problem of a jammed packing of soft spheres [Franz and Parisi(2016)]. This theory predicts the same critical behavior of the interparticle gap and force distributions and the same scaling of the coordination number versus the pressure, $\Delta z \sim p^{1/2}$, as those found for jammed packings of spherical particles.

1.4 Numerical Confirmations of the Mean-Field Theory of Jamming

Jammed systems offer a uniquely useful arena to test the predictions of the mean-field theory. Because they are athermal, one can devise experimental and numerical systems to directly measure the particle-scale properties that are predicted by the theory. Over the past decade, fruitful collaborations have emerged between theory, experiment, and numerical simulation to confirm many of the mean-field theoretical predictions in athermal jammed systems.

One of the first, and most striking, confirmations of the mean-field theory has come from the examination of the distribution of inter-particle forces, $P(f)$, in systems at jamming onset [Charbonneau *et al.*(2015)Charbonneau, Corwin, Parisi and Zamponi]. The small-force tail of the force distribution contributes significantly to the mechanical properties of a packing [Wyart(2010)]. Both the distribution of small gaps and small forces between particles determine the statistics of contact breaking and formation when a system is mechanically perturbed. The mean-field theory makes a precise prediction about the distribution of small forces. If breaking a weak contact results in a spatially *extended* soft mode, the tail of the force distribution scales as $P(f) \sim f^{\theta_e}$, where $\theta_e \approx 0.42311$. However, if breaking a weak contact results in a spatially *localized* soft mode, a

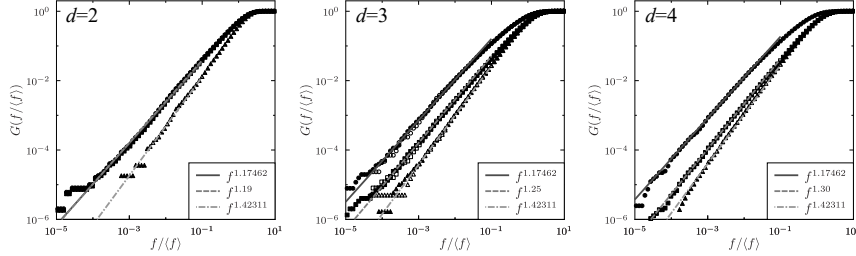


Fig. 1.3 Cumulative force distributions $G(f)$ for $d=2, 3$, and 4 , showing power-law distributions at small forces. The overall distribution (with fits shown by the dashed lines) shows evolution with spatial dimension. However, when split into *buckler* and *non-buckler* contacts, $G(f)$ for the former is well-fit by a power-law with exponent $1 + \theta_l$ and $G(f)$ for the latter is well-fit by a power-law with exponent $1 + \theta_e$ in all dimensions, in excellent agreement with the mean-field theory predictions. Figure reproduced with permission from Ref. [Charbonneau *et al.*(2015)Charbonneau, Corwin, Parisi and Zamponi] ©(2015) American Physical Society.

different argument, based on an analysis of marginal mechanical stability, predicts that the tail of the distribution will be distributed as $P(f) \sim f^{\theta_l}$, where $\theta_l \approx 0.17462$ [Lerner *et al.*(2013)Lerner, Düring and Wyart]. On the face of it, the decomposition of forces into those associated with *extended* and *localized* excitations is a substantial task. However, it suffices to recognize that the vast majority of localized forces can be associated with *bucklers*, particles that are minimally stable (with only $d + 1$ contacts), d of them nearly co-planar, and hence they have only one small contact force. As shown in Fig. 1.3 (which presents the cumulative distribution of forces, $G(f) = \int_0^f df' P(f')$), when the forces are decomposed according to this rule, the mean-field theory predictions for the small force tails are observed in spatial dimensions all the way down to $d = 2$. This surprisingly precise agreement provided strong evidence that the mean-field results are predictive in physically relevant systems.

The strength and validity of the mean-field predictions were further bolstered by a comprehensive study of the finite-size effects on jammed packings [Charbonneau *et al.*(2021)Charbonneau, Corwin, Dennis, Díaz Hernández Rojas, Ikeda, Parisi and Ricci-Tersenghi]. This work showed that the aforementioned force distribution exponents are remarkably precise in low dimensions for systems as small as $N = 256$ particles, showing essentially no finite-size effects.

One unexpectedly fruitful system of interest for studying the implications of the mean-field theory is the so-called *Gardner crystal*, consisting of

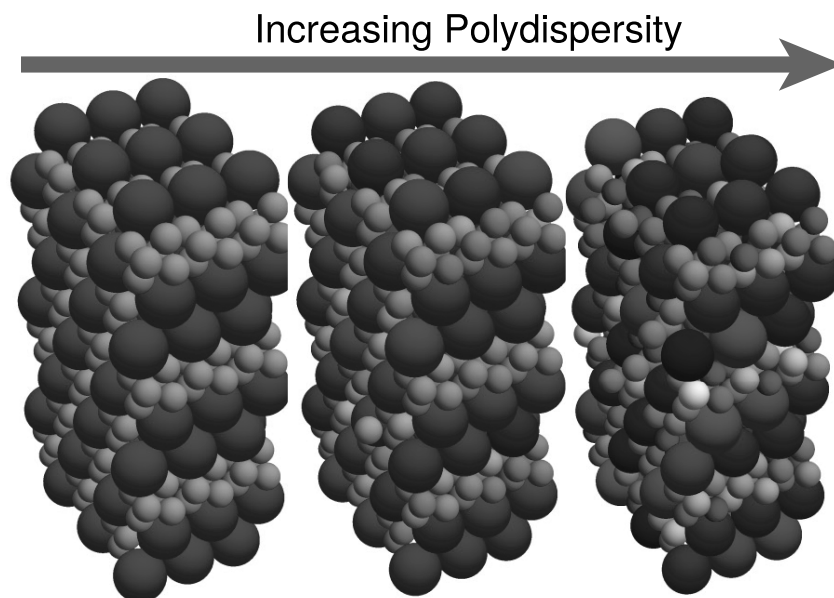


Fig. 1.4 A crystalline sphere packing with increasing amounts of polydispersity in the particle sizes, from perfectly crystalline on the left to 5% polydispersity on the right. Figure reproduced with permission from Ref. [Charbonneau *et al.*(2019)Charbonneau, Corwin, Fu, Tsekenis and van der Naald] ©(2019) American Physical Society.

slightly polydisperse spheres packed into a nearly perfect crystal, as shown in Fig. 1.4. At high temperature or low pressure, the polydispersity is effectively masked by the random motions of the particles, resulting in a solid with conventional properties. However, as the temperature is decreased or the pressure is increased, the cages around each particle shrink. Once the gaps between particles become comparable to the scale of the polydispersity, the system is forced to make choices between a hierarchy of different possible configurations, akin to what takes place in an amorphous system [Charbonneau *et al.*(2019)Charbonneau, Corwin, Fu, Tsekenis and van der Naald].

Another direct confirmation of the mean-field theory of jamming was obtained in a study of the scaling prefactors relating the pressure, packing fraction, and number of contacts in jammed systems. The mean-field theory provides predictions not only for the scaling exponents relating these quantities, but also for the prefactors themselves, as a function of the spatial dimension of the system [Parisi *et al.*(2020)Parisi, Urbani and Zamponi].

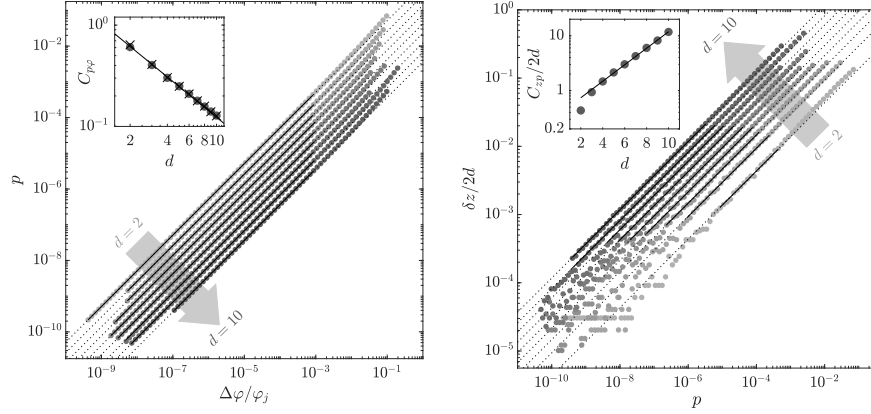


Fig. 1.5 Scaling relations between the pressure, p , and the normalized excess packing fraction, $\Delta\varphi/\varphi_j$, where φ_j is the packing fraction at jamming onset, and the excess contact number, $\delta z \equiv \Delta Z/N$ versus p . The dotted lines are best fits to the scaling relations obtained by the mean-field theory of jamming, as a function of the spatial dimension from $d = 2$ to 10. The insets show the prefactors of the scaling relations as points and the mean-field theory predictions for the prefactors as solid lines. Figure reproduced with permission from Ref. [Sartor *et al.*(2021)Sartor, Ridout and Corwin] ©(2021) American Physical Society.

Sartor, Ridout, and Corwin demonstrated through numerical simulations that these prefactor relations hold all the way down to $d = 2$ and 3 [Sartor *et al.*(2021)Sartor, Ridout and Corwin], as shown in Fig. 1.5.

While the above work demonstrates the predictive powers of the mean-field theory, recent work [Dennis and Corwin(2020)] has also directly confirmed that the energy landscape of jammed systems is consistent with full replica symmetry breaking. As a glassy system undergoes the Gardner transition entering a marginal glass state, the energy landscape results in an “ultrametric” structure for the very large number of marginally stable minima [Gardner(1985)]. Through an exhaustive search of the nearby minima in a local region of the energy landscape of jammed packings of finite size, Dennis and Corwin were able to directly measure the degree of ultrametricity of the landscape. They found that, in the large-system limit, this landscape became precisely ultrametric, with the distance to ultrametricity scaling as $N^{-1/2}$. Thus, jammed systems can be viewed as being located deep within the Gardner phase, as described by the mean-field theory.

1.5 Experimental Validations of the Mean-Field Theory of Jamming

Experimental tests of the mean-field theory have chiefly focused on the detection of signatures of the Gardner transition in driven, athermal systems that mimic thermal systems. Seguin and Dauchot [Seguin and Dauchot(2016)] constructed a granular system of vibrated disks and used it to explore the fracturing of the energy landscape as pressure is increased. An initial, *high-energy* amorphous configuration was created by confining a system of plastic disks in a fixed volume, and thus at a fixed packing fraction. Energy introduced through vibration allowed the system to make and break inter-particle contacts and explore the local energy landscape. The system was then cyclically quenched to a higher packing fraction (and thus a higher pressure) and then decompressed to the original packing fraction. The mean squared displacement of particles, Δ at the high packing fraction, as well as the mean-squared displacement between cycles, Δ_{AB} , were measured. Figure 1.6 (a) shows that these two measurements depart from one another as the quench packing fraction is increased, which is the signature of the Gardner transition in this amorphous 2D system. Xiao, Liu, and Durian made a similar measurement on a dissimilar amorphous system, also observing the clear signature of the Gardner transition [Xiao *et al.*(2022)Xiao, Liu and Durian]. Rather than using vibrated disks, this work instead used a 2D system of air-fluidized rotors, shown in Fig. 1.6 (b), constructed with five-fold symmetry to frustrate crystallization. A flexible boundary made of a chain of particles subject to a fixed tension serves to precisely control the pressure of the system, allowing measurements that can be directly compared to the Gardner transition results predicted for thermal systems (see Fig. 1.6 (b)).

The aforementioned Gardner crystal provides opportunities for experimental studies of the Gardner transition as well. Kool, Charbonneau, and Daniels constructed a 2D system of photo-elastic disks and were able to track the formation of persistent contacts as the system passed through a Gardner-like transition [Kool *et al.*(2022)Kool, Charbonneau and Daniels]. This work also showed the characteristic splitting between fluctuations within a system and fluctuations between systems at the Gardner transition (see Fig. 1.6 (c)).

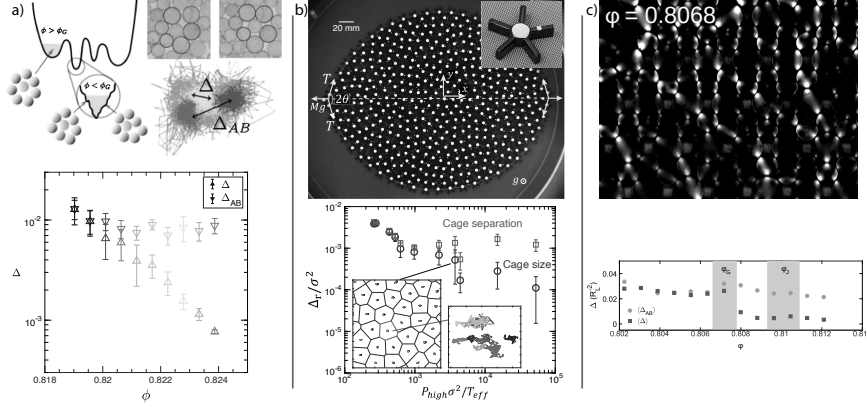


Fig. 1.6 Experimental evidence for the Gardner transition in driven, athermal disk packings, showing the characteristic splitting between Δ and Δ_{AB} at the Gardner packing fraction or pressure. a) Vibrated disk packings. b) Air-fluidized rotors. c) Slightly polydisperse crystalline configuration of photoelastic disks. Figures reproduced with permission from (a) Ref. [Seguin and Dauchot(2016)] ©(2016) American Physical Society, (b) Ref. [Xiao *et al.*(2022)Xiao, Liu and Durian] ©(2022) American Physical Society, and (c) Ref. [Kool *et al.*(2022)Kool, Charbonneau and Daniels] ©(2022) the authors.

1.6 Beyond Sphere Packings

We have presented numerical and experimental confirmations of several predictions from the mean-field theory of jamming in the context of packings of identical frictionless spherical particles, interacting via excluded volume repulsion. However, most of the materials that show jamming transitions are not composed of frictionless, spherical particles—think jelly beans, grains, and rocks. Clogging transitions, which are similar to jamming transitions, also occur in crowds of people and organisms [Bunde *et al.*(2002)Bunde, Kropp and Schellnhuber]. Moreover, many biological systems are extremely deformable, but can experience jamming transitions, like cells that form confluent tissues [Park *et al.*(2016)Park, Atia, Mitchel, Fredberg and Butler; Oswald *et al.*(2017)Oswald, Grosser, Smith and Käs]. Two additional categories of jamming transitions therefore involve packings of *non-spherical* particles and packings of *deformable* particles.

Experiments [Lu *et al.*(2016)Lu, Hidalgo, Third and Müller] and numerical simulations [Torquato and Stillinger(2010)] of jamming of non-spherical particles, such as ellipsoids [Williams and Philipse(2003)], spherocylinders [Wouterse *et al.*(2007)Wouterse, Williams and Philipse], and polyhedra [Chen *et al.*(2014)Chen, Klotz, Engel, Damasceno and Glotzer],

have probed the validity of the Maxwell criterion for determining mechanical stability [Zeravcic *et al.*(2009)Zeravcic, Xu, Liu, Nagel and van Saarloos]. Generalized to non-spherical particles, the criterion states that static packings need to possess $z = 2 \times DOF$ contacts per particle to be mechanically stable, where DOF is the number of degrees of freedom per particle [Maxwell(1864)]. As discussed earlier, the Maxwell criterion holds for sphere packings, where the number of contacts per particle is exactly $2d$ and the number of degrees of freedom per particle is equal to the spatial dimension d . Does the Maxwell criterion hold for non-spherical particles? Consider a packing of spheroids, i.e., an ellipsoid of revolution with one symmetry axis. Two degrees of freedom are required to specify the orientation of a spheroid, and three degrees of freedom are required to specify the position of the center of mass. According to the Maxwell criterion, each spheroid should possess $N_c = 2 \times (3 + 2) = 10$ contacts. However, experiments on spheroid packings clearly show that the number of contacts at jamming onset is always below ten, violating the Maxwell criterion. Therefore, jammed packings of spheroids are *hypostatic*, and possess fewer contacts than the apparent number of degrees of freedom. Subsequent numerical and experimental studies have shown that nearly all jammed packings of non-spherical particles are hypostatic.

Numerical studies have focused on investigating the mechanisms that give rise to hypostaticity in jammed packings of non-spherical particles. These studies reveal that the number of missing contacts is the same as the number of *quartic modes* [Donev *et al.*(2007)Donev, Connelly, Stillinger and Torquato]. Perturbations along these quartic modes give rise to a quartic increase in the potential energy versus the amplitude of the perturbation in the zero-pressure limit [Papanikolaou *et al.*(2013)Papanikolaou, O'Hern and Shattuck; Schreck *et al.*(2012)Schreck, Mailman, Chakraborty and O'Hern; VanderWerf *et al.*(2018)VanderWerf, Jin, Shattuck and O'Hern; Brito *et al.*(2018)Bruto, Ikeda, Urbani, Wyart and Zamponi]. Quartic modes are in fact responsible for stabilizing jammed packings of a wide range of non-spherical particles.

The structural properties of jammed packings of non-spherical particles are summarized in Fig. 1.7. Both the packing fraction and coordination number for jammed packings of non-spherical particles show non-trivial dependence on the shape parameter \mathcal{A} . In 2D, $\mathcal{A} = p^2/4\pi a$, where p is the perimeter and a is the area of the particles. In 3D, $\mathcal{A} = (4\pi)^{1/3}(3V)^{2/3}/S$, where V and S are the volume and surface area of the particles, respectively. In particular, the average packing fraction and coordination number at

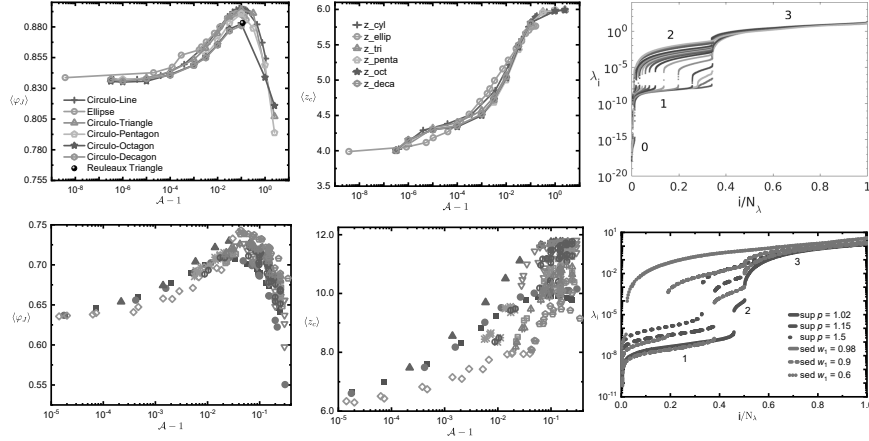


Fig. 1.7 From left to right: Average packing fraction $\langle \varphi_J \rangle$ and excess contact number $\langle z_c \rangle$ at jamming onset as a function of asphericity $\mathcal{A} - 1$ and low-frequency eigenvalues $\lambda = \omega^2$ of the dynamical matrix for jammed packings of non-spherical particles in two (top) and three (bottom) dimensions. The eigenvalues are divided in three branches: (1) quartic modes, (2) rotational modes, and (3) translational modes. Figures reproduced with permission from Refs. [VanderWerf *et al.*(2018)VanderWerf, Jin, Shattuck and O’Hern] ©(2018) American Physical Society (top panel) and Ref. [Yuan *et al.*(2019)Yuan, VanderWerf, Shattuck and O’Hern] ©(2019) Royal Society of Chemistry (bottom panel).

jamming onset follow master curves as a function of $\mathcal{A} - 1$. These results suggest that the shape parameter controls the jamming behavior of packings of non-spherical particles.

Using an extension of the perceptron model, Brito *et al.* [Brito *et al.*(2018)Brito, Ikeda, Urbani, Wyart and Zamponi] predicted the scaling of the coordination number versus the pressure and the existence of quartic modes in the VDOS for jammed packings of non-spherical particles [Schreck *et al.*(2012)Schreck, Mailman, Chakraborty and O’Hern; VanderWerf *et al.*(2018)VanderWerf, Jin, Shattuck and O’Hern]. The generalized perceptron model predicts the zero-temperature phase diagram for jammed packings of non-spherical particles in the α - σ plane, where α and σ represent the density and convexity of the obstacles on the hypersphere. (See Fig. 1.8.) The critical behavior in the presence of spherical asymmetry is substantially altered from its counterpart derived for jamming of spherical particles. In particular, different scaling exponents are predicted for the gap and force distributions, and the per-particle coordination number

scales as

$$\Delta z \sim c_A p \quad \text{with} \quad c_A \sim \mathcal{A}^{1/2}, \quad (1.5)$$

and consequently the shear modulus follows the scaling $G \sim p/\mathcal{A}^{1/2}$. These results were corroborated by previous numerical studies of jammed packings of non-spherical particles [Schreck *et al.*(2010)Schreck, Xu and O'Hern; VanderWerf *et al.*(2018)VanderWerf, Jin, Shattuck and O'Hern], proving the versatility of the mean-field theory for jamming.

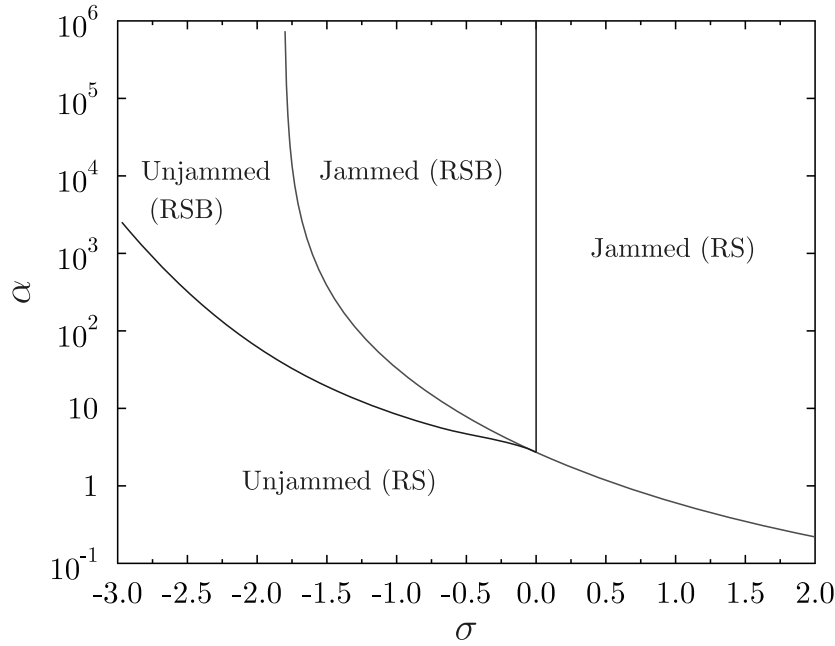


Fig. 1.8 The jamming behavior in the α - σ plane, which quantify the density and convexity of the obstacles on the N -dimensional hypersphere in the generalized perceptron model. Figure reproduced with permission from Ref. [Brito *et al.*(2018)Brito, Ikeda, Urbani, Wyart and Zamponi] ©(2018) National Academy of Sciences of the United States of America.

Particle shape has also been explored as a tool to incorporate frictional forces into the jamming framework, a direction that requires further experimental investigation [Singh *et al.*(2020)Singh, Ness, Seto, de Pablo and Jaeger]. Prior work has investigated jammed packings of particles with circular (in 2D) or spherical (in 3D) asperities on the particle surfaces [Papanikolaou *et al.*(2013)Papanikolaou, O'Hern and Shattuck]. These particles have an effective static friction coefficient μ_{eff} and the packing fraction

$\phi_J(\mu_{\text{eff}})$ and contact number z_J of packings at jamming onset mimic the behavior found for jammed packings of frictional spherical particles using the Cundall-Strack model [Cundall and Strack(1979)]. However, these packings are isostatic if all contacts between asperities are counted. Other work [Ikeda *et al.*(2020)Ikeda, Brito, Wyart and Zamponi] has also modeled friction by considering rough particle surfaces. In their studies, the amplitude and frequency of the bumps on the disk surface are continuously varied. Although this work shows a clear reduction of the coordination number and packing fraction at jamming onset with increasing static friction coefficient, it is limited to small deviations from smooth spherical shapes and it is not clear how to count contacts at concave surfaces.

The nature of the jamming transition in static packings of soft and deformable particles is much less understood. Experimental studies of aqueous colloidal suspensions have shown that particle deformability plays a crucial role in determining the mechanical properties of colloidal suspensions, leading to glassy behavior with increasing concentration [Mattsson *et al.*(2009)Mattsson, Wyss, Fernandez-Nieves, Miyazaki, Hu, Reichman and Weitz]. Colloids with larger deformations resemble strong glass-forming liquids. In contrast, harder colloids display super-Arrhenius increases in viscosity with increasing concentration, typical of fragile glasses. Other studies have shown that the shape parameter of deformable particles plays an important role in determining the onset of rigidity in cell monolayers [Bi *et al.*(2016)Bi, Yang, Marchetti and Manning].

Including particle deformability in models of jamming can describe a range of biological phenomena, such as wound healing, development of biological tissues, and macromolecular crowding. The deformable particle model (DPM) studied in 2D [Boromand *et al.*(2018)Boromand, Signoriello, Ye, O'Hern and Shattuck] and 3D [Wang *et al.*(2021a)Wang, Treado, Boromand, Norwick, Murrell, Shattuck and O'Hern], and the elastic polymer ring model [Gnan and Zaccarelli(2019)] in 2D have been developed to describe such systems. In 3D, the shape-energy function includes a volume term that represents particle compressibility, a surface tension term, and a bending energy term that assigns an energy cost to surface deformations. Studies of jammed packings of deformable particles using the DPM have shown that deformable particles possess polyhedral shapes with $\mathcal{A} \sim 1.16$ at confluence, i.e., particles deform until they completely fill all of the available space as observed in epithelia and endothelia [Mongera *et al.*(2018)Mongera, Rowghanian, Gustafson, Shelton, Kealhofer, Carn, Serwane, Lucio, Giammona and Campàs; Ilina *et al.*(2020)Ilina, Gritsenko,

Syga, Lippoldt, La Porta, Chepizhko, Grosser, Vullings, Bakker, Starruß, Bult, Zapperi, Käs, Deutsch and Friedl]. Several other models have also studied the onset of jamming in the context of confluent tissues, such as the vertex [Bi *et al.*(2014)Bi, Lopez, Schwarz and Manning] and self-propelled Voronoi [Bi *et al.*(2016)Bi, Yang, Marchetti and Manning] models. Here, unjamming transitions are strongly influenced by cell activity, which includes cell speed and persistence of the direction of motion. In recent work by Agoritsas [Agoritsas(2021)], activity has been incorporated into a Dynamical Mean-Field Theory (DMFT) for a system of infinitely-persistent particles at jamming onset. DMFT represents an important avenue of research for advancing the theory of jamming to driven and active granular systems and it has been recently applied to the perceptron model [Manacorda and Zamponi(2022)]. While still in its infancy, this direction of research could potentially result in the integration of particle shape degrees of freedom into the mean-field theory of jamming.

Our goal with this chapter was to summarize the predictions of the mean-field theory of jamming that have been confirmed by numerical simulations and experiments. Most of the confirmations have been for mean-field predictions concerning jamming of frictionless, spherical particles, while more recent work has shown confirmations of the mean-field theory of jamming for frictionless, non-spherical particles and frictional, nearly spherical particles. We also present current efforts in expanding the mean-field theory to systems that more closely resemble externally driven granular media, cell aggregates, and active colloidal suspensions. The physics of jamming is far more diverse and rich than the specific topics related to confirmations of the mean-field theory that we presented here. We direct the reader to more detailed review articles for an exhaustive description of numerical and experimental studies of jamming [Liu and Nagel(2010); van Hecke(2010); Behringer and Chakraborty(2019)] and to the book by Parisi, Urbani and Zamponi for a complete description of the jamming replica theory [Parisi *et al.*(2020)Parisi, Urbani and Zamponi].

1.7 Acknowledgements

We would like to thank all of our collaborators in the community without which this work would not have been possible. Particular gratitude goes to our editor Patrick Charbonneau and Elisabeth Agoritsas, Ada Altieri, Bulbul Chakraborty, Cameron Dennis, Andrea Liu, Peter Morse, Sid

The Jamming Transition and the Marginally Stable Solid

19

Nagel, Nidhi Pashine, Mark Shattuck, Pierfrancesco Urbani, Eric Weeks, and Francesco Zamponi. E.C. and F.A. acknowledge funding from the Simons Collaboration on Cracking the Glass Problem via Award No. 454939 and C.S.O. acknowledges funding from NSF Grant No. DMREF-2118988.

Bibliography

- Agoritsas, E. (2021). Mean-field dynamics of infinite-dimensional particle systems: Global shear versus random local forcing, *Journal of Statistical Mechanics: Theory and Experiment* **2021**, 3, p. 033501, doi:10.1088/1742-5468/abdd18.
- Altieri, A. (2018). Higher-order corrections to the effective potential close to the jamming transition in the perceptron model, *Physical Review E* **97**, 1, p. 012103, doi:10.1103/PhysRevE.97.012103.
- Aluffi-Pentini, F., Parisi, V., and Zirilli, F. (1988). A global optimization algorithm using stochastic differential equations, *ACM Transactions on Mathematical Software* **14**, 4, pp. 345–365, doi:10.1145/50063.50064.
- Arceri, F. and Corwin, E. I. (2020). Vibrational Properties of Hard and Soft Spheres Are Unified at Jamming, *Physical Review Letters* **124**, 23, p. 238002, doi:10.1103/PhysRevLett.124.238002.
- Behringer, R. P. and Chakraborty, B. (2019). The physics of jamming for granular materials: A review, *Reports on Progress in Physics* **82**, 1, p. 012601, doi:10.1088/1361-6633/aadc3c.
- Bernal, J. D. (1960). Geometry of the Structure of Monatomic Liquids, *Nature* **185**, 4706, pp. 68–70, doi:10.1038/185068a0.
- Berthier, L., Biroli, G., Charbonneau, P., Corwin, E. I., Franz, S., and Zamponi, F. (2019). Gardner physics in amorphous solids and beyond, *The Journal of Chemical Physics* **151**, 1, p. 010901, doi:10.1063/1.5097175.
- Bi, D., Lopez, J. H., Schwarz, J. M., and Manning, M. L. (2014). Energy barriers and cell migration in densely packed tissues, *Soft Matter* **10**, 12, p. 1885, doi:10.1039/c3sm52893f.
- Bi, D., Yang, X., Marchetti, M. C., and Manning, M. L. (2016). Motility-Driven Glass and Jamming Transitions in Biological Tissues, *Physical Review X* **6**, 2, p. 021011, doi:10.1103/PhysRevX.6.021011.
- Biere, A., Heule, M., and van Maaren, H. (2009). *Handbook of Satisfiability* (IOS Press), ISBN 978-1-60750-376-7.
- Boromand, A., Signoriello, A., Ye, F., O’Hern, C. S., and Shattuck, M. D. (2018). Jamming of Deformable Polygons, *Physical Review Letters* **121**, 24, p. 248003, doi:10.1103/PhysRevLett.121.248003.

- Brito, C., Ikeda, H., Urbani, P., Wyart, M., and Zamponi, F. (2018). Universality of jamming of nonspherical particles, *Proceedings of the National Academy of Sciences* **115**, 46, pp. 11736–11741, doi:10.1073/pnas.1812457115.
- Brito, C. and Wyart, M. (2006). On the rigidity of a hard-sphere glass near random close packing, *Europhysics Letters (EPL)* **76**, 1, pp. 149–155, doi:10.1209/epl/i2006-10238-x.
- Brito, C. and Wyart, M. (2009). Geometric interpretation of previtrification in hard sphere liquids, *Journal of Chemical Physics* **131**, 2, p. 024504, doi:10.1063/1.3157261.
- Bunde, A., Kropp, J., and Schellnhuber, H. J. (2002). *The Science of Disasters* (Springer Berlin Heidelberg, Berlin, Heidelberg), ISBN 978-3-642-62531-2 978-3-642-56257-0, doi:10.1007/978-3-642-56257-0.
- Cates, M. E., Wittmer, J. P., Bouchaud, J.-P., and Claudin, P. (1998). Jamming, Force Chains, and Fragile Matter, *Physical Review Letters* **81**, 9, pp. 1841–1844, doi:10.1103/PhysRevLett.81.1841.
- Chacko, R. N., Sollich, P., and Fielding, S. M. (2019). Slow Coarsening in Jammed Athermal Soft Particle Suspensions, *Physical Review Letters* **123**, 10, p. 108001, doi:10.1103/PhysRevLett.123.108001.
- Charbonneau, P., Corwin, E. I., Dennis, R. C., Díaz Hernández Rojas, R., Ikeda, H., Parisi, G., and Ricci-Tersenghi, F. (2021). Finite-size effects in the microscopic critical properties of jammed configurations: A comprehensive study of the effects of different types of disorder, *Physical Review E* **104**, 1, p. 014102, doi:10.1103/PhysRevE.104.014102.
- Charbonneau, P., Corwin, E. I., Fu, L., Tsekenis, G., and van der Naald, M. (2019). Glassy, Gardner-like phenomenology in minimally polydisperse crystalline systems, *Physical Review E* **99**, 2, p. 020901, doi:10.1103/PhysRevE.99.020901.
- Charbonneau, P., Corwin, E. I., Parisi, G., and Zamponi, F. (2015). Jamming Criticality Revealed by Removing Localized Buckling Excitations, *Physical Review Letters* **114**, 12, p. 125504, doi:10.1103/PhysRevLett.114.125504.
- Chen, E. R., Klotsa, D., Engel, M., Damasceno, P. F., and Glotzer, S. C. (2014). Complexity in Surfaces of Densest Packings for Families of Polyhedra, *Physical Review X* **4**, 1, p. 011024, doi:10.1103/PhysRevX.4.011024.
- Cundall, P. A. and Strack, O. D. L. (1979). A discrete numerical model for granular assemblies, *Géotechnique* **29**, 1, pp. 47–65, doi:10.1680/geot.1979.29.1.47.
- Dagois-Bohy, S., Tighe, B. P., Simon, J., Henkes, S., and van Hecke, M. (2012). Soft-Sphere Packings at Finite Pressure but Unstable to Shear, *Physical Review Letters* **109**, 9, p. 095703, doi:10.1103/PhysRevLett.109.095703.
- de Gennes, P. G. (1999). Granular matter: A tentative view, *Reviews of Modern Physics* **71**, 2, pp. S374–S382, doi:10.1103/RevModPhys.71.S374.
- DeGiuli, E., Lerner, E., and Wyart, M. (2015). Theory of the Jamming Transition at Finite Temperature, *The Journal of Chemical Physics* **142**, 16, p. 164503, doi:10.1063/1.4918737.
- Dennis, R. C. and Corwin, E. I. (2020). Jamming Energy Landscape is Hierarchical and Ultrametric, *Physical Review Letters* **124**, 7, p. 078002, doi:

- 10.1103/PhysRevLett.124.078002.
- Donev, A., Connelly, R., Stillinger, F. H., and Torquato, S. (2007). Underconstrained jammed packings of nonspherical hard particles: Ellipses and ellipsoids, *Physical Review E* **75**, 5, p. 051304, doi:10.1103/PhysRevE.75.051304.
- Donev, A., Torquato, S., and Stillinger, F. H. (2005). Pair correlation function characteristics of nearly jammed disordered and ordered hard-sphere packings, *Physical Review E: Statistical Physics, Plasmas, Fluids, and Related Interdisciplinary Topics* **71**, 1, p. 011105, doi:10.1103/PhysRevE.71.011105.
- Durian, D. J. (1995). Foam Mechanics at the Bubble Scale, *Physical Review Letters* **75**, 26, pp. 4780–4783, doi:10.1103/PhysRevLett.75.4780.
- Ellenbroek, W. G., Somfai, E., van Hecke, M., and van Saarloos, W. (2006). Critical Scaling in Linear Response of Frictionless Granular Packings near Jamming, *Physical Review Letters* **97**, 25, p. 258001, doi:10.1103/PhysRevLett.97.258001.
- Ellenbroek, W. G., van Hecke, M., and van Saarloos, W. (2009). Jammed frictionless disks: Connecting local and global response, *Physical Review E* **80**, 6, p. 061307, doi:10.1103/PhysRevE.80.061307.
- Franz, S., Hwang, S., and Urbani, P. (2019). Jamming in Multilayer Supervised Learning Models, *Physical Review Letters* **123**, 16, p. 160602, doi:10.1103/PhysRevLett.123.160602.
- Franz, S. and Parisi, G. (2016). The simplest model of jamming, *Journal of Physics A: Mathematical and Theoretical* **49**, 14, p. 145001, doi:10.1088/1751-8113/49/14/145001.
- Franz, S., Parisi, G., Sevelev, M., Urbani, P., and Zamponi, F. (2017). Universality of the SAT-UNSAT (jamming) threshold in non-convex continuous constraint satisfaction problems, *SciPost Physics* **2**, 3, p. 019, doi:10.21468/SciPostPhys.2.3.019.
- Gardner, E. (1985). Spin glasses with p-spin interactions, *Nuclear Physics B* **257**, pp. 747–765, doi:10.1016/0550-3213(85)90374-8.
- Gnan, N. and Zaccarelli, E. (2019). The microscopic role of deformation in the dynamics of soft colloids, *Nature Physics* **15**, 7, pp. 683–688, doi:10.1038/s41567-019-0480-1.
- Goodrich, C. P., Dagois-Bohy, S., Tighe, B. P., van Hecke, M., Liu, A. J., and Nagel, S. R. (2014). Jamming in finite systems: Stability, anisotropy, fluctuations, and scaling, *Physical Review E* **90**, 2, p. 022138, doi:10.1103/PhysRevE.90.022138.
- Goodrich, C. P., Ellenbroek, W. G., and Liu, A. J. (2013). Stability of jammed packings I: The rigidity length scale, *Soft Matter* **9**, 46, p. 10993, doi:10.1039/c3sm51095f.
- Goodrich, C. P., Liu, A. J., and Sethna, J. P. (2016). Scaling ansatz for the jamming transition, *Proceedings of the National Academy of Sciences* **113**, 35, pp. 9745–9750, doi:10.1073/pnas.1601858113.
- Hales, S., Gribelin, S., Innys, J., Innys, W., Woodward, T., Innys, W. a. J., and Woodward, T. (1727). *Vegetable Staticks, or, An Account of Some Statical Experiments on the Sap in Vegetables : Being an Essay towards a*

- Natural History of Vegetation : Also, a Specimen of an Attempt to Analyse the Air, by a Great Variety of Chymio-Statical Experiments; Which Were Read at Several Meetings before the Royal Society* (Printed for W. and J. Innys ... :—and T. Woodward, London), ISBN 978-0-356-03012-8, doi:10.5962/bhl.title.562.
- Ikeda, A., Berthier, L., and Biroli, G. (2013). Dynamic criticality at the jamming transition, *The Journal of Chemical Physics* **138**, 12, p. 12A507, doi:10.1063/1.4769251.
- Ikeda, H., Brito, C., Wyart, M., and Zamponi, F. (2020). Jamming with Tunable Roughness, *Physical Review Letters* **124**, 20, p. 208001, doi:10.1103/PhysRevLett.124.208001.
- Ilin, O., Gritsenko, P. G., Syga, S., Lippoldt, J., La Porta, C. A. M., Chepizhko, O., Grosser, S., Vullings, M., Bakker, G.-J., Starrau, J., Bult, P., Zapperi, S., Käs, J. A., Deutsch, A., and Friedl, P. (2020). Cell–cell adhesion and 3D matrix confinement determine jamming transitions in breast cancer invasion, *Nature Cell Biology* **22**, 9, pp. 1103–1115, doi:10.1038/s41556-020-0552-6.
- Kirkpatrick, S. (1984). Optimization by simulated annealing: Quantitative studies, *Journal of Statistical Physics* **34**, 5–6, pp. 975–986, doi:10.1007/BF01009452.
- Kool, L., Charbonneau, P., and Daniels, K. E. (2022). Gardner-like transition from variable to persistent force contacts in granular crystals, *arXiv preprint arXiv:2205.06794*.
- Lerner, E., DeGiuli, E., Düring, G., and Wyart, M. (2014). Breakdown of continuum elasticity in amorphous solids, *Soft Matter* **10**, 28, p. 5085, doi:10.1039/c4sm00311j.
- Lerner, E., Düring, G., and Wyart, M. (2013). Low-energy non-linear excitations in sphere packings, *Soft Matter* **9**, 34, pp. 8252–8263, doi:10.1039/C3SM50515D.
- Liu, A. J. and Nagel, S. R. (1998). Jamming is not just cool any more, *Nature* **396**, 6706, pp. 21–22, doi:10.1038/23819.
- Liu, A. J. and Nagel, S. R. (2010). The Jamming Transition and the Marginally Jammed Solid, *Annual Review of Condensed Matter Physics* **1**, 1, pp. 347–369, doi:10.1146/annurev-conmatphys-070909-104045.
- Lu, G., Hidalgo, R. C., Third, J. R., and Müller, C. R. (2016). Ordering and stress transmission in packings of straight and curved spherocylinders, *Granular Matter* **18**, 3, p. 34, doi:10.1007/s10035-016-0637-x.
- Manacorda, A. and Zamponi, F. (2022). Gradient descent dynamics and the jamming transition in infinite dimensions, *arXiv preprint arXiv:2201.01161*.
- Mattsson, J., Wyss, H. M., Fernandez-Nieves, A., Miyazaki, K., Hu, Z., Reichman, D. R., and Weitz, D. A. (2009). Soft colloids make strong glasses, *Nature* **462**, 7269, pp. 83–86, doi:10.1038/nature08457.
- Maxwell, J. C. (1864). On the calculation of the equilibrium and stiffness of frames, *The London, Edinburgh, and Dublin Philosophical Magazine and Journal of Science* **27**, 182, pp. 294–299, doi:10.1080/14786446408643668.
- Mézard, M. and Montanari, A. (2009). *Information, Physics, and Computation*

- (Oxford University Press), ISBN 978-0-19-154719-5.
- Mézard, M., Parisi, G., Sourlas, N., Toulouse, G., and Virasoro, M. (1984). Nature of the Spin-Glass Phase, *Physical Review Letters* **52**, 13, pp. 1156–1159, doi:10.1103/PhysRevLett.52.1156.
- Middleton, A. A. and Fisher, D. S. (1993). Critical behavior of charge-density waves below threshold: Numerical and scaling analysis, *Physical Review B* **47**, 7, pp. 3530–3552, doi:10.1103/PhysRevB.47.3530.
- Mongera, A., Rowghanian, P., Gustafson, H. J., Shelton, E., Kealhofer, D. A., Carn, E. K., Serwane, F., Lucio, A. A., Giammona, J., and Campàs, O. (2018). A fluid-to-solid jamming transition underlies vertebrate body axis elongation, *Nature* **561**, 7723, pp. 401–405, doi:10.1038/s41586-018-0479-2.
- Newton, I. (1848). *Newton's Principia: The Mathematical Principles of Natural Philosophy* (D. Adee).
- O'Hern, C. S., Langer, S. A., Liu, A. J., and Nagel, S. R. (2002). Random Packings of Frictionless Particles, *Physical Review Letters* **88**, 7, p. 075507, doi:10.1103/PhysRevLett.88.075507.
- O'Hern, C. S., Silbert, L. E., Liu, A. J., and Nagel, S. R. (2003). Jamming at zero temperature and zero applied stress: The epitome of disorder, *Physical Review E: Statistical Physics, Plasmas, Fluids, and Related Interdisciplinary Topics* **68**, 1, p. 011306, doi:10.1103/PhysRevE.68.011306.
- Oswald, L., Grosser, S., Smith, D. M., and Käs, J. A. (2017). Jamming transitions in cancer, *Journal of Physics D: Applied Physics* **50**, 48, p. 483001, doi:10.1088/1361-6463/aa8e83.
- Papanikolaou, S., O'Hern, C. S., and Shattuck, M. D. (2013). Isostaticity at Frictional Jamming, *Physical Review Letters* **110**, 19, p. 198002, doi:10.1103/PhysRevLett.110.198002.
- Parisi, G., Urbani, P., and Zamponi, F. (2020). *Theory of Simple Glasses: Exact Solutions in Infinite Dimensions* (Cambridge University Press), ISBN 978-1-108-12610-6.
- Park, J.-A., Atia, L., Mitchel, J. A., Fredberg, J. J., and Butler, J. P. (2016). Collective migration and cell jamming in asthma, cancer and development, *Journal of Cell Science*, p. jcs.187922doi:10.1242/jcs.187922.
- Pázmándi, F., Scalettar, R. T., and Zimányi, G. T. (1997). Revisiting the Theory of Finite Size Scaling in Disordered Systems: n Can Be Less than 2d, *PHYSICAL REVIEW LETTERS* **79**, 25, p. 4.
- Rainone, C. and Urbani, P. (2016). Following the evolution of glassy states under external perturbations: The full replica symmetry breaking solution, *Journal of Statistical Mechanics: Theory and Experiment* **2016**, 5, p. 053302, doi:10.1088/1742-5468/2016/05/053302.
- Sartor, J. D., Ridout, S. A., and Corwin, E. I. (2021). Mean-Field Predictions of Scaling Prefactors Match Low-Dimensional Jammed Packings, *Physical Review Letters* **126**, 4, p. 048001, doi:10.1103/PhysRevLett.126.048001.
- Schreck, C. F., Bertrand, T., O'Hern, C. S., and Shattuck, M. D. (2011). Repulsive Contact Interactions Make Jammed Particulate Systems Inherently Nonharmonic, *Physical Review Letters* **107**, 7, p. 078301, doi:10.1103/PhysRevLett.107.078301.

- Schreck, C. F., Mailman, M., Chakraborty, B., and O'Hern, C. S. (2012). Constraints and vibrations in static packings of ellipsoidal particles, *Physical Review E* **85**, 6, p. 061305, doi:10.1103/PhysRevE.85.061305.
- Schreck, C. F., Xu, N., and O'Hern, C. S. (2010). A comparison of jamming behavior in systems composed of dimer- and ellipse-shaped particles, *Soft Matter* **6**, 13, p. 2960, doi:10.1039/c001085e.
- Seguin, A. and Dauchot, O. (2016). Experimental Evidence of the Gardner Phase in a Granular Glass, *Physical Review Letters* **117**, 22, p. 228001, doi:10.1103/PhysRevLett.117.228001.
- Silbert, L. E., Liu, A. J., and Nagel, S. R. (2005). Vibrations and Diverging Length Scales Near the Unjamming Transition, *Physical Review Letters* **95**, 9, p. 098301, doi:10.1103/PhysRevLett.95.098301.
- Singh, A., Ness, C., Seto, R., de Pablo, J. J., and Jaeger, H. M. (2020). Shear Thickening and Jamming of Dense Suspensions: The “Roll” of Friction, *Physical Review Letters* **124**, 24, p. 248005, doi:10.1103/PhysRevLett.124.248005.
- Tkachenko, A. V. and Witten, T. A. (1999). Stress propagation through frictionless granular material, *Physical Review E* **60**, 1, pp. 687–696, doi:10.1103/PhysRevE.60.687.
- Torquato, S. and Stillinger, F. H. (2010). Jammed hard-particle packings: From Kepler to Bernal and beyond, *Reviews of Modern Physics* **82**, 3, pp. 2633–2672, doi:10.1103/RevModPhys.82.2633.
- van Deen, M. S., Simon, J., Zeravcic, Z., Dagois-Bohy, S., Tighe, B. P., and van Hecke, M. (2014). Contact changes near jamming, *Physical Review E* **90**, 2, p. 020202, doi:10.1103/PhysRevE.90.020202.
- van Hecke, M. (2010). Jamming of soft particles: Geometry, mechanics, scaling and isostaticity, *Journal of Physics: Condensed Matter* **22**, 3, p. 033101, doi:10.1088/0953-8984/22/3/033101.
- VanderWerf, K., Boromand, A., Shattuck, M. D., and O'Hern, C. S. (2020). Pressure Dependent Shear Response of Jammed Packings of Frictionless Spherical Particles, *Physical Review Letters* **124**, 3, p. 038004, doi:10.1103/PhysRevLett.124.038004.
- VanderWerf, K., Jin, W., Shattuck, M. D., and O'Hern, C. S. (2018). Hypostatic jammed packings of frictionless nonspherical particles, *Physical Review E* **97**, 1, p. 012909, doi:10.1103/PhysRevE.97.012909.
- Wang, D., Treado, J. D., Boromand, A., Norwick, B., Murrell, M. P., Shattuck, M. D., and O'Hern, C. S. (2021a). The structural, vibrational, and mechanical properties of jammed packings of deformable particles in three dimensions, *Soft Matter* **17**, 43, pp. 9901–9915, doi:10.1039/D1SM01228B.
- Wang, P., Zhang, S., Tuckman, P., Ouellette, N. T., Shattuck, M. D., and O'Hern, C. S. (2021b). Shear response of granular packings compressed above jamming onset, *Physical Review E* **103**, 2, p. 022902, doi:10.1103/PhysRevE.103.022902.
- Widom, B. (1965). Equation of State in the Neighborhood of the Critical Point, *The Journal of Chemical Physics* **43**, 11, pp. 3898–3905, doi:10.1063/1.1696618.

- Williams, S. R. and Philipse, A. P. (2003). Random packings of spheres and spherocylinders simulated by mechanical contraction, *Physical Review E* **67**, 5, p. 051301, doi:10.1103/PhysRevE.67.051301.
- Wittmer, J. P., Claudin, P., Cates, M. E., and Bouchaud, J.-P. (1996). An explanation for the central stress minimum in sand piles, *Nature* **382**, 6589, pp. 336–338, doi:10.1038/382336a0.
- Wouterse, A., Williams, S. R., and Philipse, A. P. (2007). Effect of particle shape on the density and microstructure of random packings, *Journal of Physics: Condensed Matter* **19**, 40, p. 406215, doi:10.1088/0953-8984/19/40/406215.
- Wu, Q., Bertrand, T., Shattuck, M. D., and O’Hern, C. S. (2017). Response of jammed packings to thermal fluctuations, *Physical Review E* **96**, 6, p. 062902, doi:10.1103/PhysRevE.96.062902.
- Wyart, M. (2010). Scaling of phononic transport with connectivity in amorphous solids, *EPL* **89**, 6, p. 64001, doi:10.1209/0295-5075/89/64001.
- Wyart, M. (2012). Marginal Stability Constrains Force and Pair Distributions at Random Close Packing, *Physical Review Letters* **109**, 12, p. 125502, doi:10.1103/PhysRevLett.109.125502.
- Wyart, M., Nagel, S. R., and Witten, T. A. (2005). Geometric origin of excess low-frequency vibrational modes in weakly connected amorphous solids, *EPL* **72**, 3, p. 486, doi:10.1209/epl/i2005-10245-5.
- Xiao, H., Liu, A. J., and Durian, D. J. (2022). Probing Gardner Physics in an Active Quasithermal Pressure-Controlled Granular System of Noncircular Particles, *Physical Review Letters* **128**, 24, p. 248001, doi:10.1103/PhysRevLett.128.248001.
- Yuan, Y., VanderWerf, K., Shattuck, M. D., and O’Hern, C. S. (2019). Jammed packings of 3D superellipsoids with tunable packing fraction, coordination number, and ordering, *Soft Matter* **15**, 47, pp. 9751–9761, doi:10.1039/C9SM01932D.
- Zeravcic, Z., Xu, N., Liu, A. J., Nagel, S. R., and van Saarloos, W. (2009). Excitations of ellipsoid packings near jamming, *EPL (Europhysics Letters)* **87**, 2, p. 26001, doi:10.1209/0295-5075/87/26001.